GEOPHYSICAL RESEARCH LETTERS, VOL. 23, NO. 13, PAGES 1613-1616, JUNE 15, 1996

Characteristics of 4-day oscillations trapped by the Juan de Fuca Ridge

Glenn A. Cannon

Pacific Marine Environmental Laboratory, NOAA, Seattle, Washington

Richard E. Thomson

Institute of Ocean Sciences, Sidney, B.C., Canada

Abstract. Current meter observations from different studies along the crest of the Juan de Fuca Ridge have been combined to show new features of the relatively large, broad spectral peak centered near a period of about 4 days. The coherence range of the 4-day oscillations has been extended to the extreme ends of the ridge, and the trapped waves appear to propagate northward along the entire length of the ridge at about 1 m/s. Spectral amplitudes are about double on the south end compared to the north end, and a recent model for bottom-trapped subinertial waves over topography shows this may be due to variations in ridge width [*Allen and Thomson*, 1993]. New observations show coherence between temperatures and currents near the South Cleft vent field and suggest 4-day oscillations can play a major role in the local advection of hydrothermal plumes. These observations combined with earlier results demonstrate that 4-day oscillations are a significant ridge-trapped feature, and they suggest that other ridges may be important in transmitting energy over much longer distances.

Introduction

The Juan de Fuca Ridge is a hydrothermally active spreading center off the west coast of North America (Figure 1). The ridge extends about 400 km from 44.5°N to 48.0°N and is a region of complex topography with numerous offset ridge segments and connecting seamount chains. Depths of the crest vary from about 2100 to 2400 m, except at Axial Seamount which shoals to about 1500 m at the junction of the Cobb-Eickleberg seamount chain. Plumes emanating from hydrothermal venting on the ridge have been studied for more than 10 years, and sites of major interest have included the Cleft Segment in the south and the Endeavour Segment in the north. Cleft Segment is relatively long and narrow, and Endeavour is shorter and broader.

Numerous year-long current measurements have been made concentrating on two main sites separated by about 370 km near 48°N [*Thomson et al.*, 1990] and south of 45°N [*Cannon et al.*, 1991]. A dominant feature in these observations was a persistent broad-band current oscillation with a period in the 3–8 day range centered on approximately 4-days (hereafter called 4-day). Characteristics on the two ends of the ridge included maximum amplitude at the crest decreasing both horizontally and vertically, clockwise rotation, intermittency, and winter intensification, all of which are commensurate with surface storm generation. Observations also showed northward propagation at about 1 m/s along the crest from the southern end to the Axial-Brown Bear sill. A recent model of subinertial oscillations over a ridge has demonstrated trapping with preferential amplification of the clockwise rotary component [*Allen and Thomson*, 1993]. The theory was applied primarily to diurnal tides, but it has application to weather-band currents.

The purpose of this paper is to combine the overlapping parts of our earlier observations near the extreme ends of the ridge to

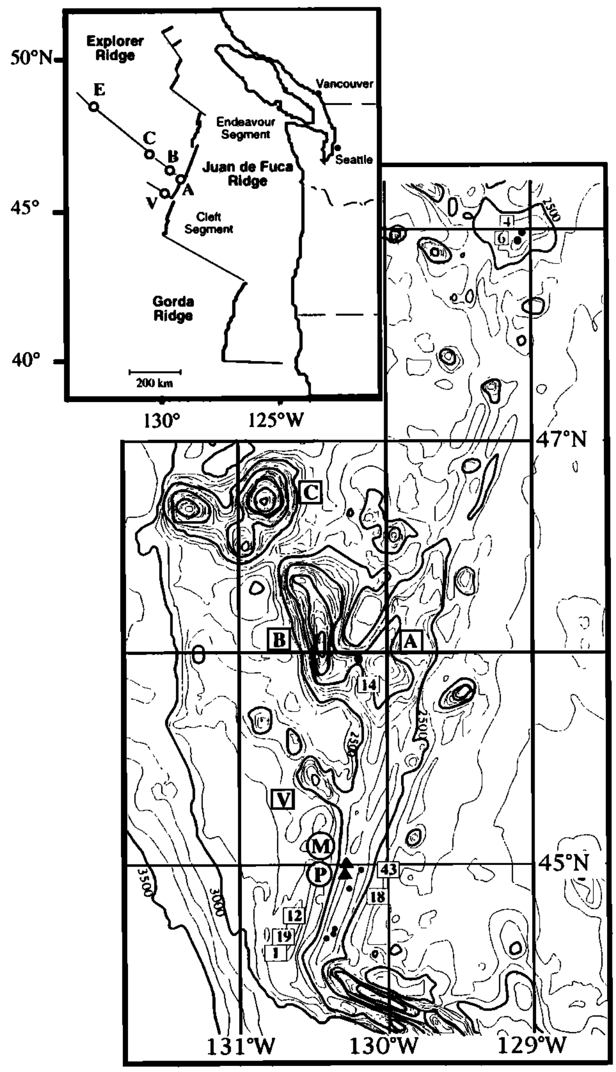

Figure 1. Chart of the Juan de Fuca Ridge. Moorings (numbered) are shown by dots, and Monolith (M) and Pipe Organ (P) vents are shown by triangles near 45°N. The contour interval is 100 m with 2500 m darkened. Seamounts noted are Eickleberg (E), Cobb (C), Brown Bear (B), Axial (A), and Vance (V).

Paper number 96GL01370
0094-8534/96/96GL-01370$05.00

provide additional understanding of the 4-day feature, partly in light of the Allen and Thomson model. In addition, we present new observations that show 4-day oscillations are sufficiently large to affect the location of plumes from hydrothermal vents.

Observations

Current meter observations on the northern end of the ridge have been made around the Endeavour Segment vent site (Figure 1, moorings 4 and 6; hereafter just numbers), while the southern ones were from several locations along the Cleft Segment. The earliest observations on Cleft were near three vents about midway along the segment at 44.6°N (between 1 and 12) and the more recent ones (43) were near the vent field (M and P) that was discovered in 1990 just south of 45°N. Concurrent observations were made on the two segments with a single current meter in 1984–85 (1 and 4) for 280 days starting in September. More extensive arrays were deployed on the two segments in 1986–87 that included vertical distribution of instruments at two sites (12 and 6) and other nearby moorings. Overlapping sampling at the two segments occurred for 260 days starting in September. Observations in 1987–88 on south and north Cleft (19 and 18) and near 46°N on the Axial-Brown Bear sill (14) first showed propagation characteristics along the southern half of the ridge [*Cannon et al.*, 1991]. An off-axis mooring (43) deployed in 1990–91 about 2.4 km southeast of Monolith vent (M) will be used to show what we believe are 4-day effects on plume oscillations. All measurements were made

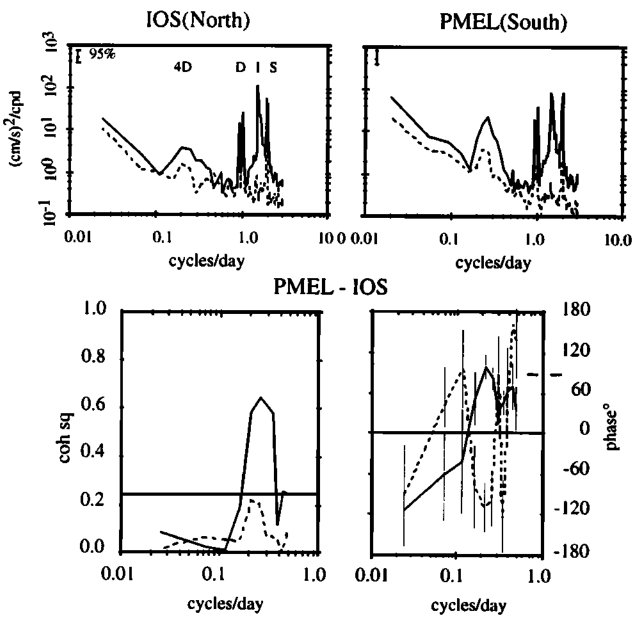

Figure 2. Top: Rotary energy density spectra for 260 days in 1986-87 near 2000 m on the north (mooring 6, Figure 1) and south (mooring 12) ends of the Juan de Fuca Ridge. Peaks identified are at 4-day (4D), diurnal (D), inertial (I), and semidiurnal (S) periods. Solid curves are clockwise, dashed are counterclockwise, and 95% confidence limits are shown for 24 degrees of freedom.

Bottom: Rotary coherence squared and phase between currents on the south (12) and north (6) ends of the ridge (spectra at left). Solid curves are clockwise, and 95% confidence limits are the horizontal line near 0.2 coherence and the vertical lines at each phase for 24 dof. Ticks at 90° phase indicate south leads north for the 4-day oscillations.

with Aanderaa current meters on subsurface taut wire moorings. Sampling and analysis techniques were described in our earlier papers.

Spectra from Endeavour and Cleft segments were similar, showing peaks at tidal, inertial, and 4-day periods (Figure 2). The broad 4-day peaks were significant at the 95% level extending over a half-power range of about 3–5 days, and the oscillations primarily exhibited a clockwise rotation. Since the oscillations have a bandwidth of 0.133 cpd (i.e., periods of 3–5 days), the duration of the events, measured by the inverse, is about 7.5 days. The peak spectral amplitudes for the concurrent observations were significantly larger in the south (20 $(cm/s)^2$/cpd) than in the north (4 $(cm/s)^2$/cpd). Spectra from winter showed a significant increase in energy, and the 4-day peaks were about double the yearly magnitudes. Amplitudes in both locations were larger in other years. In 1984–85 they were about double those in Figure 2 for 1986–87. In 1987–88 amplitudes over the southern end of the ridge also were about twice as large as 1986–87. The range from various years of nonconcurrent observations was 15–40 and 3–7 $(cm/s)^2$/cpd, respectively, in the south and north.

The 4-day oscillations at the two ends of the ridge (12 and 6; separation about 370 km) were significantly coherent at the 95% confidence level with a coherence-squared (hereafter, coherence) of 0.65 in clockwise rotation (Figure 2). The phase difference at the coherence peak was about 90° with the south end leading the north. Assuming the period is exactly 4 days and that the relatively large distance between observation sites is between one and two cycles, the calculated propagation speed and wave length would be about 0.9 m/s and 300 km, respectively. If it was assumed that the phase difference was associated with the first cycle, the propagation speed would be 4.3 m/s, which is unreasonably large for topographically trapped waves. Concurrent observations in 1984 (1 and 4; separation about 380 km) had a higher coherence of 0.8 and a phase difference of about 30°. The calculated northward propagation speed and wave length were 1.0 m/s and 350 km, respectively. The 4-day oscillations in both years were maximum during the 3-month period of December–February, and the propagation speeds for that interval (0.9 and 1.1 m/s) basically were the same as for the total records. Higher 4-day coherences (0.9) occurred in 1987–88 between the two closely spaced moorings on the crest of Cleft Segment (19 and 18; separation about 20 km) and between Cleft and the Axial-Brown Bear sill (19 or 18 and 14; separation about 120 km) [*Cannon et al.*, 1991]. The northward propagation speeds between those sites on the southern part of the ridge were the same (1.0 m/s) as those calculated here for the total length of the ridge.

Temperature Variations

A single mooring (43) was deployed on Cleft Segment to monitor currents and temperature during 1990–91. It was located on the east side of the ridge axis 2.4 km from the newly discovered Monolith vent to not interfere with planned submersible observations. It provided one of the first opportunities to study possible nearby effects from a vent when not aligned along-axis with the dominant flow. The mean flow over the 8 months was 2–3 cm/s southward along the ridge, and low-pass filtered current fluctuations were up to 10 cm/s along-axis and 3–4 cm/s across the ridge (Figure 3). Simultaneous temperature oscillations were 0.05–.07°C at 2200 m, but temperature was relatively uniform at 2000 m, which was above the plume. The

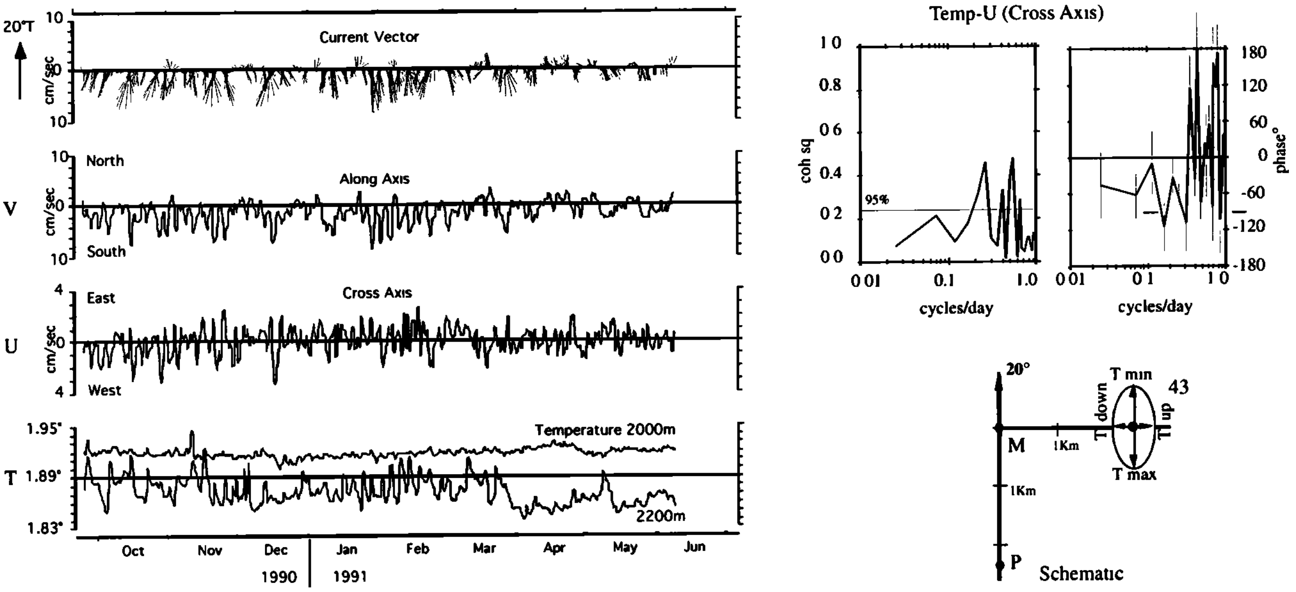

Figure 3. Left: Currents and temperature near bottom (2200 m) and temperature above plume level (2000 m) at mooring 43 (Figure 1), 2.4 km southeast of Monolith vent (M). Data are 35-hr low-pass filtered, and currents are shown both as vectors and components oriented along 20°T.

Right, top: Coherence squared and phase between temperature and cross-axis flow in the plume at 2200 m. Confidence intervals as in Figure 2. Ticks at −90° phase indicate temperature lags eastward cross-axis flow (toward 110°T) for the 4-day oscillations.

Right, bottom: Schematic representation of 4-day clockwise rotating currents at mooring 43, shown relative to Monolith (M) and Pipe Organ (P) vents. Temperature rises during 2-days with eastward flow component (−90° phase in top figure). Oval indicates north-south flows are larger.

temperature and current oscillations were largest in October–November and in January–February, and the current vector time series showed rotary flow characteristics of the 4-day oscillations. Spectra showed a significant 4-day peak in both temperature and flow.

The 4-day coherence between temperature and the cross-axis flow was small (0.5), but significant at the 95% confidence level, and the phase was about 90° with temperature lagging eastward flow (Figure 3). A comparable coherence peak also occurred at a period of about 2 days. The 4-day coherence between along-axis flow and temperature was larger (0.7, not shown) with temperature lagging northward flow by about 180°. Because the 4-day flow rotates clockwise, temperature increased during the transition from northward to southward flow during cross-axis flow to the east (shown schematically in Figure 3), and the interpretation is that the occurrence of warmer temperatures at the mooring indicated the presence of plume water. The cross-axis maximum flow was about 4 cm/s (average about 2 cm/s), and the 2.4 km from Monolith vent to the mooring could be traversed in about half of the 2 days of eastward flow. The phases were not exactly 90° and 180°, suggesting the situation may be a little more complicated because of the existence of Pipe Organ vent (P) as well as Monolith (M). However, the temperature increases of 0.05–.07°C at mooring 43 are comparable to anomalies derived from towed plume observations simultaneous with moored instrument measurements [*Baker and Cannon*, 1993]. Coherence between moored current and temperature observations in that study were similar to those presented here, although the phases were somewhat more complicated possibly because of the relative orientation between vents and moorings. Also, the topography on the crest is relatively flat, and no tows on the Juan de Fuca Ridge have ever suggested temperature increases or decreases occurring due to downwelling or upwelling, respectively.

Discussion

The observations presented here combined with earlier results indicate that 4-day weather-band oscillations were significantly coherent along the entire 400-km length of the Juan de Fuca Ridge. They propagated northward along the crest with near-bottom energy levels that were always larger on the southern end. A recent theory of subinertial oscillations across simplified ridge topography can account for some of the characteristics [*Allen and Thomson*, 1993]. The model showed bottom-trapped oscillations and amplification of the clockwise rotary component of velocity over the ridge. Amplification was a function of bottom slope, ridge height, oscillation frequency, and inversely of ridge width, and it required a cross-ridge component to the oscillations. Although their study emphasized diurnal tides, they showed application to the weather-band oscillations that had a cross-ridge component about 30° to the east of the ridge. They also noted that the amplification of the weather band would be considerably less than the diurnal band partly because the weather band is broad and intermittent, and the phases were random from one event to the next.

The larger amplification over the southern end can be explained by the *Allen and Thomson* [1993] theory as a function of ridge width with all other variables being about the same for the two portions of the ridge. Endeavour Segment is part of a region of broad substructures and Cleft Segment is a relatively long, narrow feature (Figure 1). Allan and Thomson used a width of 10 km for Endeavour. However, for comparison we used the 2500-m contour widths of about 15 and 5 km, respectively. In fact, Endeavour may be relatively wider depending on the number of topographic substructures included. Thus, the amplification at Cleft would be at least 3 times that at Endeavour, which is about what was observed (Figure 2).

The 4-day oscillations propagated northward from Cleft to Endeavour immediately over the crest, as did those in *Cannon et al.* [1991] along Cleft Segment and from Cleft Segment to Axial Volcano. Trapped subinertial oscillations of *Allen and Thomson* [1993] traveled around a ridge as a wave with shallow water on the right. However, *Kilworth* [1989] has shown asymmetric topographic waves can propagate along one side of a ridge and extend onto the ridge crest. There were insufficient observations along both sides of the ridge in these studies to deduce opposing propagation on the two sides. The only observations of southward propagation of 4-day oscillations along the east side were electric field observations away from the steep topography that showed a speed of about 3 m/s with an uncertainty factor of 2 [*Chave et al.*, 1989].

An alternate mechanism might be that the 4-day oscillations are linked to local wind generation, with the high coherence between currents arising from the large spatial coherence of the wind field. Currents would be locally generated but would appear to have along-axis propagation characteristics simply because of the wind stress coherence along the ridge. *Luther* [1995] also suggested another transmission mechanism due the disjointed nature of the ridge segments. Excitation of ridge resonance on one segment could excite a neighboring segment, and if this resulted in some energy loss at each segment, the south to north energy decrease could also be explained.

A major obstacle for northward propagation of a wave is Axial seamount (Figure 1), and observations in 1987–88 showed northward amplification of the 4-day oscillations (10–15 to 25 cm/s) from Cleft Segment to the Axial-Brown Bear sill [*Cannon et al.*, 1991]. Thus, it seems possible there is a wave propagating northward along the west side and crest of the southern ridge (over two segments) that has sufficient energy to shoal and cross the 1800-m Axial sill. Its amplification there may be inversely related to the relatively narrow topography of the pass.

The generation of the 4-day oscillations is beyond the scope of this paper, but it is becoming reasonably clear that they are due to local storms. *Cannon et al.* [1991] showed significant coherence between local wind stress and 4-day currents. *Mofjeld et al.* [1996] described weather-induced bottom-pressure fluctuations with about 5-day periods at Axial Volcano that they suggested were generated more by local atmospheric forcing than by propagation of oceanic Rossby waves westward from the coast (less than a Rossby radius away). *Luther et al.* [1990] showed local atmospheric forcing of bottom barotropic velocity for 4- and 6-day periods at the BEMPEX site (40°N, 163°W) using coherence maps with wind stress curl over a large region in the central North Pacific. Their observations were in agreement with stochastic forcing of oceanic motions [*Muller and Frankignoul*, 1981]. Further understanding of the generation process near the Juan de Fuca Ridge would require a similar study.

An important local implication of the 4-day oscillations that may be applicable to other vent systems on other ridges is their effect on the dispersal of hydrothermal effluents. Although it is obvious that plumes move with the flow, e.g., tidal currents, these are the first known observations to show a 4-day oscillation can have a major effect. Submersible operations on Endeavour Segment in June 1995 occurred during a stormy period with large changes in plume direction, but the lack of current observations precluded determination of plume rotation characteristics (G. Lebon, PMEL/NOAA, personal communication). The observations at mooring 43 east of Monolith vent suggest that plumes can circulate about their source with a 4-day period, and they may or may not be located at the particular site (43) on a particular day (Figure 3). There is no east wall along the rift valley near Monolith vent, perhaps making spreading easier in that direction. However, the height of the plume extended well above the west wall, suggesting that the rotary characteristics could be over both sides of the ridge. Laboratory studies have shown that plumes can generate clockwise vortices that can become unstable and break off from the source [*Helfrich and Battisti*, 1991]. Perhaps the 4-day clockwise oscillations also contribute to this process.

Finally, the extension of the coherence range to the entire length of the Juan de Fuca Ridge has potential application to other ridges. Trapped energy may be able to travel much longer distances along other more extensive midocean ridges.

Acknowledgments. We are particularly grateful to David Pashinski, PMEL, who assisted with everything from field work to data analysis, our other support staffs, the ships *Discoverer* and *Endeavour*, and very helpful reviewers. Support for GAC was from the NOAA Vents Program. PMEL contribution 1673.

References

Allen, S. E., and R. E. Thomson, Bottom-trapped subinertial motions over midocean ridges in a stratified rotating fluid, *J. Phys. Oceanogr.*, *23*, 566–581, 1993.

Baker, E. T., and G. A. Cannon, Long-term monitoring of hydrothermal heat flux using moored temperature sensors, Cleft Segment, Juan de Fuca Ridge, *Geophys. Res. Lett.*, *20*, 1855–1858, 1993.

Cannon, G. A. and D. J. Pashinski, Circulation near Axial seamount, *J. Geophys. Res.*, *95*, 12,813–12,828, 1990.

Cannon, G. A., D. J. Pashinski, and M. R. Lemon, Middepth flow near hydrothermal venting sites on the southern Juan de Fuca Ridge, *J. Geophys. Res.*, *96*, 12,815–12,831, 1991.

Chave, A. D., J. H. Filloux, D. S. Luther, L. K. Law, and A. White, Observations of motional electromagnetic fields during EMSLAB, *J. Geophys. Res.*, *94*, 14,153–14,166, 1989.

Helfrich, K. M., and T. M. Battisti, Experiments on baroclinic vortex shedding from hydrothermal plumes, *J. Geophys. Res.*, *96*, 12,511–12,518, 1991.

Kilworth, P. D., Transmission of a two-layer coastal Kelvin wave over a ridge, *J. Phys. Oceanogr.*, *19*, 1131–1148, 1989.

Luther, D. S., Waves trapped to discrete topography: Existence and implications, *Proc. 8th Hawaiian Winter Workshop*, edited by P. Muller and D. Henderson, Univ. Hawaii at Manoa, pp. 43–56, 1995.

Luther, D. S., A. D. Chave, J. H. Filloux, and P. F. Spain, Evidence for local and non-local barotropic responses to atmospheric forcing during BEMPEX, *Geophys. Res. Lett.*, *17*, 949–952, 1990.

Mofjeld, H. O., F. I. Gonzalez, and M. C. Eble, Subtidal bottom pressure fluctuations observed at Axial Seamount in the northeastern continental margin of the Pacific Ocean, *J. Geophys. Res.*, in press, 1996.

Muller, P., and C. Frankignoul, Direct forcing of geostrophic eddies, *J. Phys. Oceanogr.*, *11*, 287–308, 1981.

Thomson, R. E., S. E. Roth, and J. Dymond, Near-inertial motions over a mid-ocean ridge: Effects of topography and hydrothermal plumes, *J. Geophys. Res.*, *95*, 7261–7278, 1990.

G. A. Cannon, PMEL/NOAA, 7600 Sand Point Way NE, Seattle, WA 98115-0070 (e-mail: cannon@pmel.noaa.gov)

R. E. Thomson, IOS, PO Box 6000, Sidney, BC, V8L 4B2, Canada (e-mail: rick@ios.bc.ca)

(Received September 24, 1995; revised April 11, 1996; accepted April 23, 1996.)